ELSEVIER

Robotics and Autonomous Systems 35 (2001) 131–142

Robotics and Autonomous Systems

www.elsevier.com/locate/robot

Physics-based modelling of human skin colour under mixed illuminants

Moritz Störring*, Hans Jørgen Andersen, Erik Granum

Computer Vision and Media Technology Laboratory, Aalborg University, Niels Jernes Vej 14, DK-9220 Aalborg, Denmark

Abstract

Skin colour is an often used feature in human face and motion tracking. It has the advantages of being orientation and size invariant and it is fast to process. The major disadvantage is that it becomes unreliable if the illumination changes. In this paper, skin colour is modelled based on a reflectance model of the skin, the parameters of the camera and light sources. In particular, the location of the skin colour area in the chromaticity plane is modelled for different and mixed light sources. The model is empirically validated. It has applications in adaptive segmentation of skin colour and in the estimation of the current illumination in camera images containing skin colour.

Keywords: Skin colour segmentation; Varying illuminant colour; Skin colour modelling

1. Introduction

There are many computer vision applications which automatically detect and track human faces and human motion. These applications are as diverse as: human–computer interfaces, surveillance systems, and automatic camera men.

Skin colour is an often used feature in such systems [5,6,10–13]. It is mostly used as an initial approximate localisation and segmentation of faces or hands in the camera image. This reduces the search region for other more precise and computationally expensive facial feature detection methods. Thus, it is important that the output of the skin colour segmentation gives reliable information. Advantages of using skin colour are that it is size and orientation invariant, and fast to process. It is suitable for real time systems [6,13].

A problem with robust skin colour detection arises under varying lighting conditions. The same skin area appears as two different colours under two different illuminations. This is a well known problem in colour vision and there are several *colour constancy* methods trying to cope with this. However, until now no generic method has been found [8].

The appearance of skin depends on the brightness and the colour of the illumination. The dependency on the brightness can be resolved by transforming into a chromatic colour space as done by, e.g., Schiele and Waibel [13]. McKenna et al. [10] report a face tracking system where the skin colour segmentation algorithm adapts to the skin chromaticity distribution using adaptive Gaussian mixture models. They can track a face moving relative to fixed light sources, i.e. they can cope with changing illumination geometry, but no tests under significant changes of the illuminant colour are reported.

The dependency on the illuminant colour is usually not taken into account in skin colour segmentation, despite the fact that the skin colour chromaticities

* Corresponding author.
E-mail addresses: mst@vision.auc.dk (M. Störring), hja@vision.auc.dk (H.J. Andersen), eg@vision.auc.dk (E. Granum).

0921-8890/01/$ – see front matter
PII: S0921-8890(01)00122-1

may change drastically when changing the illumination colour. Only recently the changes of skin colour under different illumination colours were investigated [16,17]. Störring et al. [17] show that it is possible to model skin colour for different illuminant colours with a good approximation.

This paper investigates theoretically and experimentally the colour image formation process, in particular with respect to human skin colour, using one or two illumination sources.

We first review general models for reflection and for illumination sources. Then, the reflections of skin colour are modelled. A series of experiments is done in order to compare the measured with the modelled data.

The specific problems addressed are:

- How well can skin colour reflections be modelled for a range of illumination sources and for a range of different humans with varying skin colours due their genetic backgrounds.
- How well does the modelling of illumination sources by Blackbody radiators apply in this application context.
- How well does the modelling of mixed illumination sources apply for skin colour analysis.

The answer to the first problem provides insight about the potential of using skin colour as a general robust method in a range of computer vision applications when humans appear in the scenario. The second problem evaluates the possibilities of using simple models for frequently used illumination sources. The last problem is extremely important for the practical applications of skin colour analysis, as mixed illumination is a typical situation in every day live.

2. Modelling colour reflections and light sources

The image formation process using a colour video camera can be modelled by spectral integration. Knowing the spectrum of the incoming light, the spectral sensitivities of the camera's sensing elements, and the spectral transmittance of filters in front of the sensing elements one can model, e.g., the red, green, and blue (RGB) pixel values. The incoming light results from the spectrum of the light source and the reflectance characteristic of the reflecting material. This is often described by the Dichromatic Reflection Model. In this work, the reflecting material is human skin. The following sections explain and model the above mentioned process and discuss the illumination of everyday scenarios.

2.1. Dichromatic reflection model

The light $L(\theta, \lambda)$ reflected from an object is determined by its reflectance and the light it is exposed with. It is a function of the wavelength λ and the photometric angles θ including the viewing angle e, the phase angle g, and the illumination direction angle i, see Fig. 1. For dielectric non-homogeneous materials this is often modelled by the Dichromatic Reflection Model [15], which describes the reflected light $L(\theta, \lambda)$ as an additive mixture of the light L_S reflected at the material's surface (*interface* or *surface reflection*) and the light L_B reflected from the material's body (*body*, *diffuse*, or *matte reflection*):

$$L(\theta, \lambda) = m_S(\theta)L_S(\lambda) + m_B(\theta)L_B(\lambda), \quad (1)$$

where $m_S(\theta)$ and $m_B(\theta)$ are geometrical scaling factors for the surface and body reflections, respectively [9]. For materials with high oil or water content the light reflected on the surface has approximately the same spectral power distribution as the light it is exposed with, i.e. it has the same colour as the illuminant. This is categorised as the Dichromatic Reflection Model Type I, also known as the Neutral Interface Reflection (NIR) assumption [19].

The light, which is not reflected at the surface, penetrates into the material body where it is

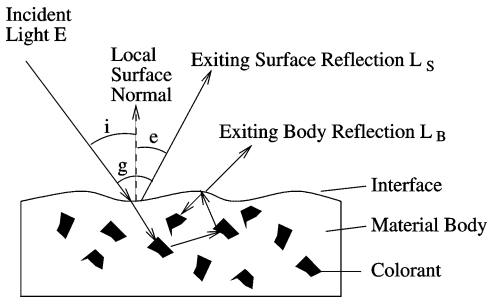

Fig. 1. Photometric angles and reflection components from a non-homogeneous dielectric material [9].

scattered and selectively absorbed at wavelengths that are characteristic of the material. Some fraction of the light arrives again at the surface and exits the material, Fig. 1. The body reflection provides the characteristic colour of the material.

The reflected light L_S and L_B from the surface and body components is the product of the incident light spectrum E and the material's spectral surface reflectance ρ_S and body reflectance ρ_B, respectively: $L_S(\lambda) = E(\lambda)\rho_S(\lambda)$ and $L_B(\lambda) = E(\lambda)\rho_B(\lambda)$. The spectra of light sources and skin reflectance will be described later.

The measured colours by a camera also depend on the characteristics of the used camera. While the Dichromatic Reflection Model describes light reflection using the continuous light spectrum, the camera sensing device uses only a finite set of samples to describe the spectrum [9], usually the colours red, green and blue (RGB). Sample measurements are obtained by filtering the light spectrum and integrating over this filtered spectrum, which is referred to *spectral integration*:

$$\boldsymbol{C}_{\mathrm{RGB}} = \int_{\lambda_v} L(\theta, \lambda)\boldsymbol{f}_{\mathrm{RGB}}(\lambda)\,\mathrm{d}\lambda, \tag{2}$$

where $\boldsymbol{f}_{\mathrm{RGB}}(\lambda)$ are the spectral sensitivities of the red, green and blue sensing elements of the camera (*tristimulus characteristic*, see Fig. 2 for an example). $\boldsymbol{C}_{\mathrm{RGB}}$ is a three element vector of sensing element responses, i.e. the RGB pixel values. The integration is done over the spectrum λ_v where the camera is sensitive. Using the red, green and blue sensing elements reduces the infinite vector space to a three-dimensional space.

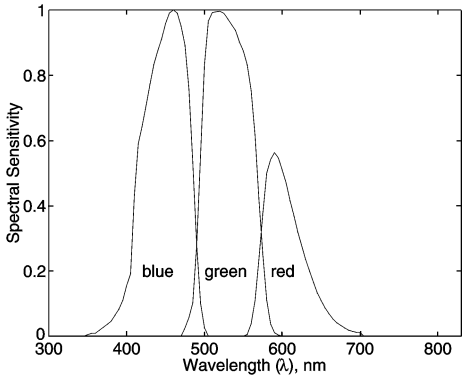

Fig. 2. Spectral sensitivities of the JAI CV-M90 3CCD colour video camera.

In this space the reflections $\boldsymbol{C}_{\mathrm{RGB}}$ from a material's surface are modelled by the Dichromatic Reflection Model as consisting of a body vector $\boldsymbol{C}_{\mathrm{body}}$ and a surface vector $\boldsymbol{C}_{\mathrm{surf}}$, Fig. 3. These two span a plane in the RGB space, called the Dichromatic plane. All RGB pixel values of the material's surface lie in this plane [9].

For analysing the colour of the reflected light, independent of the scale of intensity, it is convenient to transform a colour vector $\boldsymbol{C}_{\mathrm{RGB}}$ to its corresponding *chromaticity* $\boldsymbol{c}_{\mathrm{rgb}}$, i.e., to the "pure colours". This is done by normalising the colour vector elements (R, G, B) with their first norm $(N = R + G + B)$:

$$r = \frac{R}{N}, \qquad g = \frac{G}{N}, \qquad b = \frac{B}{N}. \tag{3}$$

That means that $r + g + b = 1$, a mapping from 3D to 2D space. All chromaticities lie on a plane, the *chromaticity plane*, illustrated by the dash-dotted line on Fig. 3. Knowing just two of the three chromaticities determines the third, therefore only the r and g chromaticities will be used in the following figures.

The intersection line of the Dichromatic plane and the chromaticity plane is called the *Dichromatic Line* in the following. The Dichromatic line connects the body- and the surface-reflection chromaticities, $\boldsymbol{c}_{\mathrm{body}}$ and $\boldsymbol{c}_{\mathrm{surf}}$ in Fig. 3. The body chromaticity is the "pure

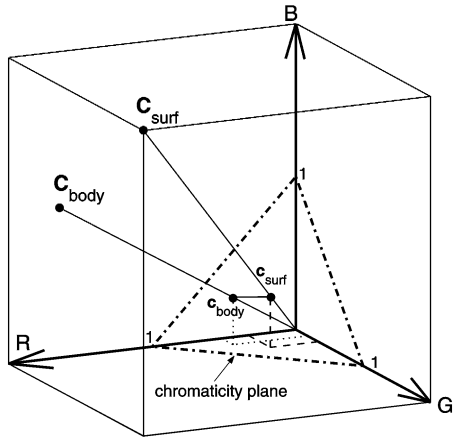

Fig. 3. RGB colour cube and the chromaticity plane. Reflections from a material are illustrated as a *body* $\boldsymbol{C}_{\mathrm{body}}$ and a *surface* $\boldsymbol{C}_{\mathrm{surf}}$ vector, respectively. Their mapping on the chromaticity plane is illustrated.

colour" of the material, here the skin. The surface chromaticity is equal to the illuminant's chromaticity.

2.2. Light sources and their approximation by Blackbody radiators

In the previous section, it was explained that the colour appearance of an object is determined by its reflectance and the light it is exposed with. This section will focus on commonly used indoor and outdoor light sources, e.g. daylight, fluorescent light, or tungsten filament light bulbs. The light source characteristics connected with the colour appearance will be described.

The colour of a light source is defined by its spectral composition. Figs. 4 and 5 show the relative radiant power distributions of several light sources over the visible wavelengths. The spectral composition of a light source may be described by the *correlated colour temperature* (CCT) and the *general colour rendering index* R_a [4,20].

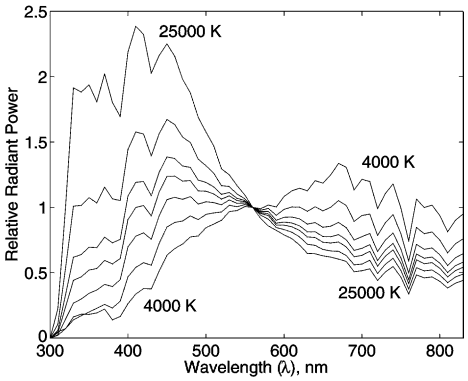

Fig. 4. Relative spectral radiance of daylight [4] normalised at $\lambda = 560$ nm. CCT varying from 4000 to 25000 K.

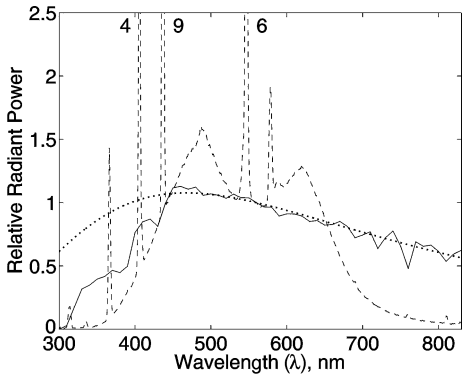

Fig. 5. Spectra of a blackbody radiator (dotted), daylight (solid), and fluorescent light (dashed) all with a CCT of 6200 K and normalised at $\lambda = 560$ nm.

The CCT of a light source is relating to the temperature of a Blackbody radiator emitting light of a similar spectral composition. It is measured in Kelvin (K). A spectrum with a low CCT has a maximum in the radiant power distribution at long wavelengths, which gives the material a reddish appearance, e.g. sunlight during sunset and low power electric light bulbs. A light source with a high CCT has a maximum in the radiant power distribution at short wavelengths and gives the material a bluish appearance, e.g., diffuse skylight and special fluorescent lamps. Fig. 4 includes these two extrema for daylight.

The general colour rendering index of a light source determines the quality of the colour appearance of objects in comparison with their appearance under a reference light source. Usually the reference source is a Blackbody source, which is also the case in the following examples. The higher R_a the better the correspondence. R_a can be maximally 100 [20]. Fluorescent lamps may have low values for R_a, thus the object will have a "unnatural" colour appearance. Electric light bulbs have mostly tungsten as filament material. The spectral distribution of tungsten is approximately like that of a Blackbody radiator, thus $R_a = 100$. Fig. 5 shows the spectra of a Blackbody radiator, daylight, and a fluorescent lamp, all having a CCT of 6200 K. One can see that the daylight spectrum is close to the Blackbody spectrum where as the fluorescent lamp spectrum deviates significantly from the blackbody spectrum. The fluorescent lamp has a $R_a = 90$, the daylight has a $R_a = 99.6$.

Fig. 6 shows the r and g chromaticities of the three light spectra shown in Fig. 5. A 3700 K Blackbody radiator is used as *canonical illuminant*. The canonical illuminant is the light source for which the camera is white balanced. That means that the camera response to this light source is $R = G = B$ and for the chromaticities that $r = g = b = \frac{1}{3}$.

The chromaticities of daylight and fluorescent light have only a small deviation from the Blackbody radiator with the same CCT. Finlayson and Schaefer [7] measured 172 light sources, including daylights and fluorescent. They report that the illuminant

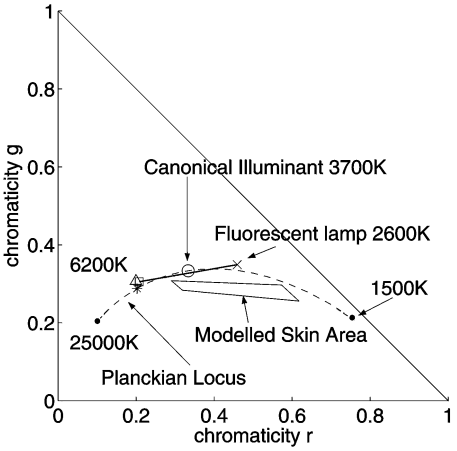

Fig. 6. Modelled *rg*-chromaticities of the spectra shown in Fig. 5: fluorescent (△), daylight (□), and Blackbody (∗). The solid line shows all mixtures of a 2600 K fluorescent lamp and 6200 K daylight, which are varying their relative intensity. The skin area modelled for this mixture of illumination is explained in Section 3.2.

chromaticities fall on a long thin band in the chromaticity plane which is very close to the Planckian locus of Blackbody radiators. General purpose light sources might therefore be approximated by Blackbody radiators of the same CCT.

2.3. Mixed illumination

Realistic indoor and outdoor scenes usually have more than one source of illumination. These can illuminate locally different areas, which can be treated locally as single source illuminated as described above. Some areas might be illuminated by more than one source. This case will be modelled in the following paragraphs.

Outdoors there could be a mixture of direct sunlight, which has a CCT of around 5700 K, and diffuse skylight, which may have a CCT up to 25 000 K. Indoors there may be a mixture of several electric lamps and daylight. Traditional filament lamps have CCTs between 2500 K and 3000 K [1], while fluorescent lamps provide mostly diffuse ambient illumination with CCTs between 2600 K and 4000 K. Fluorescent lamps with higher CCTs are only used in special applications. Most halogen spots have CCTs around 3100 K [1]. Daylight entering through a window may give direct or ambient light with usually higher CCTs.

The mixture of light spectra is additive [14]. The straight solid line in Fig. 6 shows the modelled illuminant chromaticities which can occur if the light of a 2600 K fluorescent lamp with constant intensity is mixed with intensity varying daylight (CCT = 6200 K). The daylight's intensity may vary in this example from $\frac{1}{100}$ of the fluorescent lamp's radiant power up to a factor 100 of the fluorescent lamp's radiant power. In other words, this simulates an everyday indoor environment illuminated by fluorescent light and daylight which is changing its intensity, e.g. due to the use of curtains.

3. Modelling skin colour

3.1. Reflectance of human skin

Skin is composed of a thin surface layer, the *epidermis*, and the *dermis*, which is a thicker layer placed under the epidermis. *Surface reflection* of skin takes place at the epidermis surface. It is approximately $\rho_{\text{surf}} = 5\%$ of the incident light independent of its wavelength [3]. The rest of the incident light (95%) is entering the skin where it is absorbed and scattered within the two skin layers and eventually reflected (*body reflectance*). The epidermis mainly absorbs light, it has the properties of an optical filter. The light is transmitted depending on its wavelength and the melanin concentration in the epidermis. In the dermis the light is scattered and absorbed. The absorption is mainly dependent on the content of blood and its ingredients such as haemoglobin, bilirubin, and beta-carotene. The optical properties of the dermis are basically the same for all humans. The skin colour related to different genetic backgrounds is, thus, determined by the epidermis transmittance, which depends mainly on its melanin concentration. The variation of the blood content of the dermis is independent of the genetic background.

Fig. 7 shows spectral reflectance curves of human skin [3,20]. The uppermost is representative for normal Caucasian skin, the middle one for Caucasian skin right after sunburn (*erythematous*, which gives the skin a reddish appearance), and the lower one for Negro skin. The two spectral reflectance curves of Caucasian

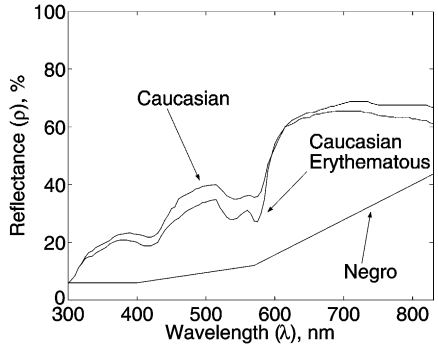

Fig. 7. Spectral reflectance curves of human skin for normal Caucasian [3], erythematous Caucasian (sunburn) [3], and dark Negro skin [20].

skin in Fig. 7 are the lower and upper extrema of the reddish appearance, which is due to the blood content of the dermis [12]. The normal Caucasian and the Negro define the range of the shade of the skin (brownish), which is due to the melanin concentration in the epidermis.

3.2. Modelling of the skin colour chromaticities

The surface and body chromaticities of the skin can be modelled using the reflectance curves of skin, the spectrum of the illumination the skin is exposed with, and the camera characteristics. Fig. 8 shows

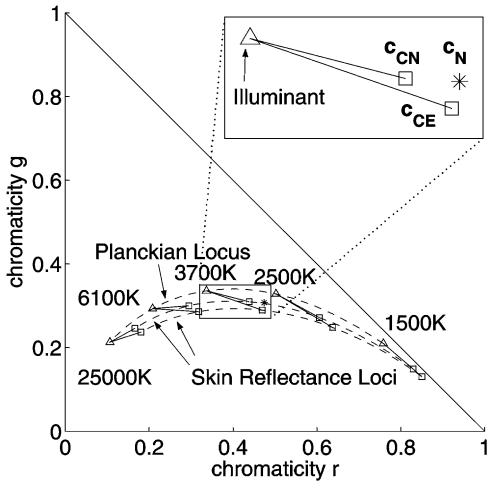

Fig. 8. Modelled illuminant and body reflection chromaticities of skin with Dichromatic lines for a number of Planckian illuminants.

the *rg*-chromaticities of a number of Blackbody illuminants ranging from 1500 to 25000 K (Planckian locus), illustrated by triangles (△). The figure is modelled for a Blackbody radiator with a CCT = 3700 K as canonical light source (white balance source). Two body reflection chromaticities, illustrated by squares (□), are modelled for each illuminant using the Caucasian reflectance curves from Fig. 7 in Eq. (2). These two chromaticities are called $\boldsymbol{c}_{\mathrm{CN}}$ and $\boldsymbol{c}_{\mathrm{CE}}$ for Caucasian *normal* and Caucasian *erythematous*. The solid lines connecting the illuminant and body chromaticities are the Dichromatic lines. According to the Dichromatic Reflection Model, skin colour chromaticities of a Caucasian subject are located in the area spanned by the three chromaticities — illuminant, Caucasian normal, and Caucasian erythematous.

In the previous section it was mentioned that the two Caucasian reflectance curves in Fig. 7 define the extrema of the reddish appearance of Caucasian skin, and that the surface reflection of skin is only 5% [3]. It is, thus, expected, that most of the Caucasian skin colour reflections lie in a plane in the RGB space, which is spanned by the two vectors of the body reflection chromaticities $\boldsymbol{c}_{\mathrm{CN}}$ and $\boldsymbol{c}_{\mathrm{CE}}$. In the chromaticity plane $\boldsymbol{c}_{\mathrm{CN}}$ and $\boldsymbol{c}_{\mathrm{CE}}$ describe a line. For other skin colours, e.g. Asian or Negro, the respective reflectance curves have to be used.

The asterisks (∗) in Fig. 8 show the body reflectance chromaticity for Negro skin $\boldsymbol{c}_{\mathrm{N}}$ (modelled with the Negro reflectance curve in Fig. 7) under the 3700 K Blackbody illumination. Compared to the changes of the chromaticities due to illumination colour changes the difference between $\boldsymbol{c}_{\mathrm{CN}}$ and $\boldsymbol{c}_{\mathrm{N}}$ is small. The body reflectance chromaticities of all other shades of skin are located between $\boldsymbol{c}_{\mathrm{CN}}$ and $\boldsymbol{c}_{\mathrm{N}}$. In order to model the range of reddish appearance a normal and an erythematous reflectance curve is required for each shade of skin. As such a set of reflectance curves was not yet available to the authors, a method, recently proposed by Ohtsuki and Healey [12], was used to synthesise skin reflectance spectra from Caucasian to Negro skin as a function of the melanin concentration.

3.3. Skin colour and mixed illumination

In Section 2.3, the illuminant chromaticities resulting from mixed light sources were modelled.

The spectra of a fluorescent lamp and varying daylight were additively mixed, Fig. 6. The figure shows also all possible skin chromaticities resulting from body reflections of skin under this illumination. They are obtained in the same way as the body reflection chromaticities under single illumination by spectral integration. The skin chromaticities are expected to be enclosed by this straight area. This might be used to constrain the search area for skin colour in the chromaticity plane.

4. Image acquisition

For the experimental test of the skin colour model images are taken from several faces under different illuminations.

The images are captured with a JAI CV-M90 3CCD colour video camera equipped with a Fudjinon wide angle lens and connected to a Silicon Graphics Sirius or a FlashBus Integral Technologies frame-grabber. No automatic gain control or automatic white balancing are used and the gamma correction is set to one. The lens opening and the shutter speed are manually adjusted to make use of the dynamic range of the camera. Fig. 2 shows the spectral sensitivities of the CV-M90 camera.

The different illuminations were realised with four fluorescent lamps (Philips TLD 927, 940, 950, 965), having the CCTs 2600 K, 3680 K, 4700 K, and 6200 K. The spectra of these lamps are provided from Philips and additionally measured with a J & M TIDAS spectrometer. The measured spectra where used to calculate the CCTs. Fig. 5 shows an example of a measured spectrum of a fluorescent lamp (dashed line). The fluorescent lamps are running with high frequency (>24 kHz) in order to avoid the 50 Hz flicker of the power system. Fig. 9 shows the setup for the image acquisition.

JAI recommends a standard illumination of 2000 lux for the CV-M90 camera using an opening of $F = 5.6$. This illuminance is available in approximately 1.5 m distance to the lamps. Fluorescent lamps provide their full luminous flux 20 minutes after they are switched on. Therefore all the lamps are switched on during the acquisition and covered when not in use (Fig. 9). The fluorescent lamp with a CCT of 3680 K was used as canonical light source, i.e. to white balance the camera.

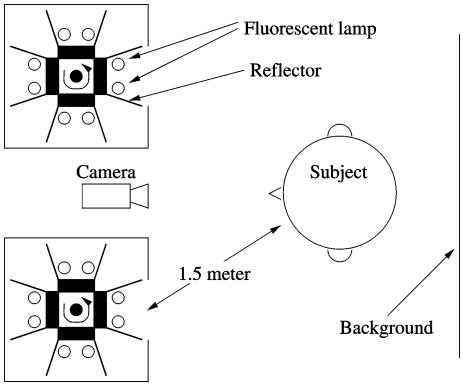

Fig. 9. Top view of the setup for capturing images of peoples faces under lighting with different and mixed CCT.

Indoor images of eight subjects coming from a variety of countries (China, Iran, Cameroun, Latvia, Greece, Spain, Denmark, and India) and hence with different skin colours were taken. An example image is shown in Fig. 10. Five images of each subject were taken using the lamps in the order 940, 927, 965, 950, 940. Two images are taken at the CCT = 3680 K, one at the beginning and one at the end of a set of images as a reproducibility test to make sure that the subject's skin properties did not change, e.g., more or less reddish at the end of the sequence.

Fig. 10. Image acquired by the setup shown in Fig. 9. Examples of colour images are available at http://www.cvmt.auc.dk/~mst/ras.html.

4.1. Images under mixed illumination

In Section 2.3, a mixture of daylight and fluorescent light was modelled. In order to simulate such a mixture images of faces were taken illuminated with a mixture of different fluorescent lamps. This was done by setting two fluorescent lamps with different CCTs in the same casing, e.g. a 6200 K lamp together with a 2600 K lamp. Hence, 10 different illuminations were available, six with mixed CCTs and four with a single CCT.

5. Comparison of measured and modelled data

The images were hand segmented into skin areas and non-skin areas. The skin areas are used as skin colour measurements. First images taken under a single illumination colour will be investigated for known illumination spectra and for blackbody radiator modelled illumination. At the end of this section images taken under mixed illumination will be discussed.

5.1. Single known illumination

Fig. 11 shows the mean values of the measured skin colour distributions in the chromaticity plane for the eight subjects under the four different illuminations. The four areas, illustrated by the solid lines, are the modelled body reflectances of human skin ranging from light Caucasian to dark Negro (melanin concentration) and from pale to reddish (blood content), respectively. For the upper boundary a reflectance curve from a very light Caucasian is used, which was provided by the "physics-based face database for colour research" [16] from Oulu University, Finland. The four measured light source spectra where used for the modelling.

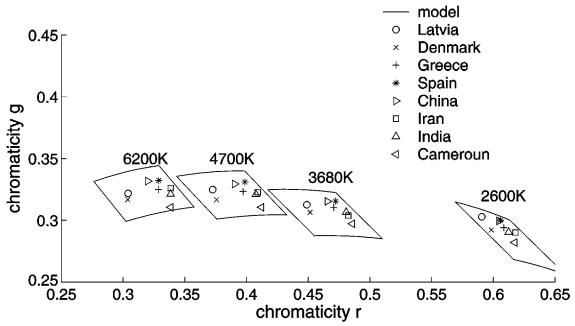

Fig. 11. Chromaticity plane with modelled skin colour areas and mean values of the measured skin colour distributions under the four different CCTs as described in Section 4. The nationalities of the subjects are indicated by the different symbols, see legend.

The measurements lie inside the modelled skin colour areas, as one would expect for known light spectra and this wide range of modelled skin colour. The relative structure of the distribution of the mean values looks similar for the different illuminations, it changes about the same as the structure of the modelled area changes its form. The lighter subjects (Caucasians) are closer to the illuminant chromaticity (white) that the darker ones as it was shown in Fig. 8. The calculated area for the lowest CCT (2600 K) is slightly lower relative to the measurements than the other areas. The images taken at 2600 K have relatively high values for the red component and rather low ones for the blue component of the skin, respectively. Thus, this deviation might be due to non-linearities of the camera, or due to the use of product specifications for the spectral sensitivities of the camera instead of using measures of the camera actually used.

The mean values of the three skin colour distributions shown in Fig. 12 are extrema in Fig. 11 (Latvia, China, and Cameroun). The modelled skin colour area (solid lines) is the same as that in Fig. 11. All mean values of measured skin colour clusters are inclosed by the modelled area.

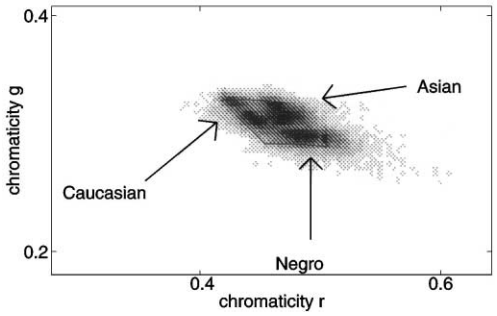

Fig. 12. Skin colour distribution in the chromaticity plane of images taken at CCT = 3680 K. The solid line indicates the skin area, modelled with a large range of melanin. The images contain skin pixels of one Caucasian (Latvia), one Asian (China), and one Negro (Cameroun) subject. Approximately 10000 skin pixels per subject.

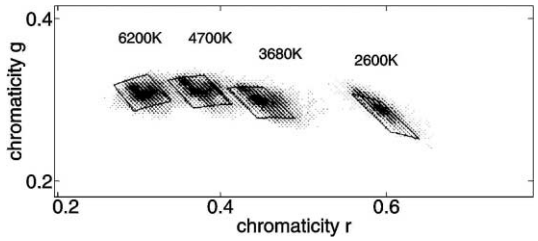

Fig. 13. Skin colour distribution of a Caucasian (Latvia) subject under four different illuminations. The solid line shows the modelled skin colour area adapted to the subject.

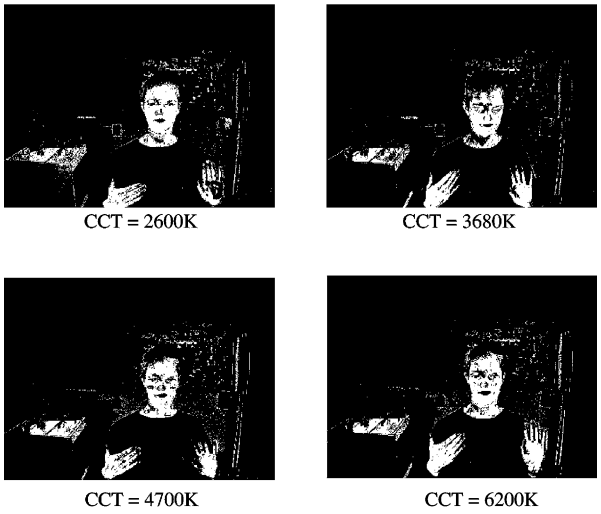

Fig. 14. Images segmented using the model shown in Fig. 13. The top left image is the segmentation from the image shown in Fig. 10.

The Caucasian skin colour distribution is composed of two distributions. A smaller distribution on the upper left side and a bigger one below, see also Fig. 13. The upper left distribution is due to the "whiter" skin areas such as the neck, and the lower due to the rather red cheeks of the subject. The Caucasian subject has more variance in the reddishness (due to variations in the blood content) where as the Negro subject has more variance in the direction depending on the melanin concentration.

Fig. 13 shows the skin colour distributions of a light Caucasian subject. The solid line is the modelled skin area, adapted to the subject by changing the range of melanin concentration and using the same reflectance curves as above. The adaption is done for the canonical illuminant at CCT $=$ 3680 K. The skin colour areas for the other CCTs are modelled using the same parameters except the spectrum of the light source, which is changed to the respective ones. It can be seen that the modelled area changes its shape as the measured skin colour distribution does.

The modelled skin areas shown in Fig. 13 were used to do a segmentation in the chromaticity space of the respective images, i.e. if the chromaticity of a pixel falls in the modelled area it is segmented as skin colour. The segmented images are shown in Fig. 14. It can be seen that very red areas, especially the cheeks, are not always correctly segmented, e.g. the image taken at a CCT $=$ 4700 K. Also very pale/white areas, such as the neck of the subject, are not correctly segmented. These false negatives could be avoided by choosing another melanin range and other reflectance curves which include more white and red areas. This would give more false positives, which are already present in the segmentation shown in Fig. 14. The large area of false positives in the lower left of the images is a wooden surface, which has the same chromaticities as the neck of the subject. The noisy false positives occur mostly at object edges, on the notice board and the poster behind the subject, which purposely contains skin colour.

This shows that using this simple colour model can give few false negative. It also shows that there are many objects which have the same chromaticities as skin or chromaticities very closed to those of skin. A robust segmentation of human skin will only be possible using context sensitive methods and/or in combination with other feature, e.g. motion, as reported, e.g. by Crowley et al. [6], McKenna et al. [10] and Schiele and Waibel [13].

5.2. Blackbody modelling of illumination

Fig. 15 shows the same skin colour measurements as Fig. 11, but the skin areas are modelled using Blackbody radiators instead of the measured spectra. Particularly the area modelled for 2600 K is too low in the green component, but also the areas for 4700 K and 6200 K are slightly too low in the green component. This is due to the deviations of the Blackbody radiators' spectra from the corresponding (same

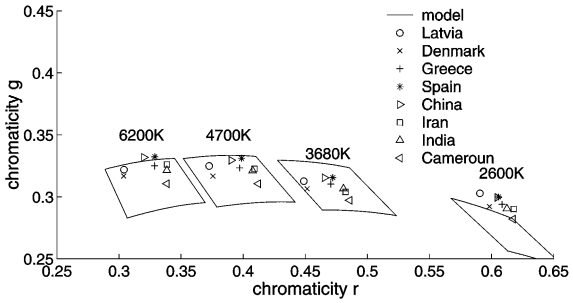

Fig. 15. Mean values of measured skin colour distribution as shown in Fig. 11. Skin colour areas are modelled using Blackbody radiators instead of the measured spectra.

CCT) fluorescent lamps' spectrum. It can be seen in Fig. 16 for the 2600 K and the 6200 K lamps that the chromaticities of the Blackbody radiators are slightly lower that those of the fluorescent lamps. The red component, on the other hand, fits nearly as well as the ones modelled using measured light spectra, Fig. 11. Thus, using Blackbody modelling for the illumination gives an accurate estimation of the red component, but the green component needs some alternative compensation in order to be used, e.g., for segmentation.

5.3. Mixed illumination

In Fig. 6, all mixtures of 2600 K fluorescent light and 6200 K daylight were modelled. The corresponding body reflections of skin colour are also shown in the chromaticity plane.

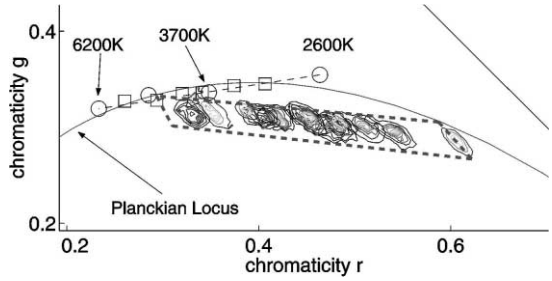

Fig. 16. Measured illuminant (○: single CCT, □: mixed CCTs) and skin colour chromaticities under single and mixed illumination. The dashed line is the modelled skin area for a mixture of 2600 K and 6200 K fluorescent light.

Fig. 16 shows the skin colour distributions of a Caucasian subject in images taken under different mixtures of illumination, as described in Section 4.1. The circles (○) illustrate measurements of single CCT illuminant colours and the squares (□) measurements of the mixed illuminant colours. These measurements were obtained from images of a Barium Sulphate plate. Barium Sulphate has an approximately constant reflectance over all visible wavelengths and reflects thus the colour of the illuminant. The measurements of the single CCT illuminant colours form a straight line. All measurements of the mixed CCT illuminant colours lie on this line as well.

The dashed lines illustrate a skin colour area, which is modelled for the two fluorescent lamps with 2600 and 6200 K, varying their relative intensities. The measured distributions of skin colour chromaticities form a linear structure as the light sources do. All cluster centres are enclosed by the modelled skin colour area. Thus, even for this mixture of CCTs, the search area for skin colour can be reduced to a rather small area in the chromaticity plane.

6. Conclusions

In the previous sections it was shown that it is possible to model human skin colour under changing and mixed illuminations. Indoor images of eight people with different skin colours under four different CCTs and mixtures of these confirm this. Body reflections of human skin are modelled by spectral integration using the spectral sensitivities of the camera, spectral reflectance curves of human skin, and the relative spectral radiance of the light sources. The spectral reflectance curves of skin are synthesised from curves taken from the literature [3,16,20] using a method proposed in [12]. Measured light spectra and blackbody radiators approximation were used. The use of measured spectra gave good approximations under single and mixed illuminations. Even under unknown relative intensities of the mixed illumination, the possible skin colours can be reduced to a small search area in the chromaticity plane (Fig. 16). The approximation by Blackbody radiators give accurate estimates in the red component but needs alternative compensation in the green component.

The skin colour model may provide the basis for a wide range of applications such as adaptive segmentation of skin colour.

In future work an adaptive skin colour segmentation using the modelling presented in this article and in [2] in combination with the illuminant estimation reported in [18] will be developed. Tests will be done using images from skin in cluttered environments and outdoors. Skin with other properties than facial skin like the palm of the hands and lips should be investigated.

Acknowledgements

We would like to thank all the persons who participated in the image acquisition, and would like to thank the European Communities TMR research network SMART II, Contract No. ERBFMRX-CT96-0052, for supporting this research.

References

[1] OSRAM Lichtprogramm, Product Catalogue, 1998.
[2] H.J. Andersen, E. Granum, Classifying illumination condition from two light sources by colour histogram assessment, Journal of the Optical Society of America A 17 (4) (2000) 667–676.
[3] R.R. Anderson J. Hu, J.A. Parrish. Optical radiation transfer in the human skin and applications in in vivo remittance spectroscopy, in: R. Marks, P.A. Payne (Eds.), Bioengineering and the Skin, MTP Press, Cambridge, MA, 1981, pp. 253–265 (Chapter 28).
[4] Anonymous. Method of measuring and specifying colour rendering properties of light sources, Technical Report CIE 13.3, Commision Internationale de L'Eclairage (CIE), 1995.
[5] C. Chen, S.-P. Chiang, Detection of human faces in colour images, IEE Proceedings on Vision Image and Signal Processing 144 (6) (1997).
[6] J.L. Crowley, J. Coutaz, F. Berard, Things that see, Communications of the ACM 43 (3) (2000) 54–64.
[7] G. Finlayson, G. Schaefer, Single surface colour constancy, in: Proceedings of the Seventh Color Imaging Conference, Scottsdale, AZ, November 1999, pp. 106–113.
[8] B. Funt, K. Barnard, L. Martin, Is machine colour constancy good enough, in: H. Burkhardt, B. Neumann (Eds.), Proceedings of the Fifth European Conference on Computer Vision, Freiburg, Germany, June 1998, pp. 445–459.
[9] G.J. Klinker, S.A. Shafer, T. Kanade, A physical approach to color image understanding, International Journal of Computer Vision 4 (1) (1990) 7–38.
[10] S.J. McKenna, S. Gong, Y. Raja, Modelling facial colour and identity with Gaussian mixtures, Pattern Recognition 31 (12) (1998) 1883–1892.
[11] T.B. Moeslund, E. Granum, Multiple cues used in model-based human motion capture, in: Proceedings of the Fourth IEEE International Conference on Automatic Face- and Gesture-Recognition, Grenoble, France, March 2000, pp. 362–367.
[12] T. Ohtsuki, G. Healey, Using color and geometric models for extracting facial features, Journal of Imaging Science and Technology 42 (6) (1998) 554–561.
[13] B. Schiele, A. Waibel, Gaze tracking based on face-color, in: M. Bichsel (Ed.), Proceedings of the International Workshop on Automatic Face- and Gesture-Recognition, Zurich, Switzerland, June 1995.
[14] S. Shafer, Describing light mixtures through linear algebra, Journal of the Optical Society of America A 72 (2) (1982) 299–300.
[15] S.A. Shafer, Using color to separate reflection components, Color Research and Application 10 (4) (1985) 210–218.
[16] M. Soriano, E. Marszalec, M. Pietikäinen, Color correction of face images under different illuminants by RGB eigenfaces, in: Proceedings of the Second International Conference on Audio- and Video-based Biometric Person Authentication, Washington, DC, March 1999, pp. 148–153.
[17] M. Störring, H.J. Andersen, E. Granum, Skin colour detection under changing lighting conditions, in: H. Araujo, J. Dias (Eds.), Proceedings of the Seventh International Symposium on Intelligent Robotic Systems, Coimbra, Portugal, July 1999, pp. 187–195.
[18] M. Störring, H.J. Andersen, E. Granum, Estimation of the illuminant colour from human skin colour, in: Proceedings of the Fourth IEEE International Conference on Automatic Face- and Gesture-Recognition, Grenoble, France, March 2000, pp. 64–69.
[19] S. Tominaga, Dichromatic reflection models for a variety of materials, Color Research and Application 19 (4) (1994) 277–285.
[20] G. Wyszecki, W.S. Stiles, Color Science: Concepts and Methods, Quantitative Data and Formulae, Wiley, New York, 1982.

Moritz Störring studied Electronical Engineering at the Technical University of Berlin, Germany, and at the Institut National Polytechnique de Grenoble, France. He graduated in 1998 in Berlin. Since April 1998, he has been employed as a Research Assistant at the Computer Vision and Media Technology Laboratory, Aalborg University, Denmark, within the European TMR project SMART II. His research interests include colour vision, outdoor computer vision, face detection, and vision based human–computer interaction. He is

currently working towards a Ph.D. on human skin colour modelling and detection.

Hans Jørgen Andersen has received a Ph.D. degree from the Computer Vision and Media Technology Laboratory, Aalborg University, 2001, within the field Outdoor Computer Vision. Prior to his Ph.D., he has received a B.Sc. in Mechanical Engineering from Horsens Technical College, 1990, and worked as a Research Assistant at the Norwegian Centre for Ecological Agriculture. After his Ph.D., he has worked as Research and Development Manager at Eco-Dan A/S introducing the first commercial system for computer vision supported guidance of agricultural machinery. Currently, he is with the Technology and Innovation Department at Siemens Mobile Phones, Pandrup, Denmark.

Erik Granum is Professor of Information Systems and Head of CVMT, Computer Vision and Media Technology Laboratory (Lab. of Image Analysis), at Aalborg University, Denmark, where he came in 1983. He got his B.Sc. in 1967, worked in industry, M.Sc. in 1973, Ph.D. in 1981, and worked for the British MRC in Edinburgh. He has been co-ordinator of several national and international research projects and networks in computer vision (including VAP, Vision as Process), and partner of many others. He is founding member of I3NET, a main partner of projects on Virtual Theatre and Visual Data Mining, partner of EU-network VIRGO, and co-ordinator of EU-project PUPPET, the "Educational Puppet Theatre of Virtual Worlds". He was a main actor in the establishment of a multimedia and virtual reality centre at Aalborg University. His research interests cover pattern recognition, motion analysis, continually operating vision systems, colour vision, vision guided multimedia interfaces, visualisation, virtual reality, and autonomous agents.